Fire resistance of concrete-filled high strength steel tubular columns

Ke Wang [a], Ben Young [b,*]

[a] *Guangdong Provincial Key Laboratory of Durability for Marine Civil Engineering, College of Civil Engineering, Shenzhen University, Shenzhen, PR China, and AECOM Asia Co. Ltd, Hong Kong*
[b] *Department of Civil Engineering, The University of Hong Kong, Pokfulam Road, Hong Kong*

Abstract

The main objective of this study is to investigate the effects of high strength structural steel on the fire resistance of concrete-filled steel tubular (CFST) columns under constant axial load using finite element analysis. A 3-D finite element model was developed to carry out both the numerical heat transfer and nonlinear stress analyses. The concrete-steel interface model was carefully considered in the finite element model. The initial geometric imperfections of the columns were also considered in the finite element model. The results obtained from the finite element analysis have been verified against experimental results, and showed that the finite element model can accurately predict fire resistance of the CFST columns. Furthermore, an extensive parametric study was performed to investigate the behaviour and strength of CFST circular columns. The parameters included the column dimensions, steel strength, concrete strength, loading ratio, different type of aggregate and moisture contents of the concrete. The column time-temperature and time-axial shortening curves were evaluated. It is shown that the diameter and strength of concrete have a relatively larger influence than the strength of steel on the fire resistance time of the CFST columns. At the same load ratio, the fire resistance is generally decreased with higher steel strength, and increased with the lower concrete strength. However, under the same load, the fire resistance of the CFST columns with the tubes yield strength of 690 MPa showed significant improvement than those steel tubes having yield strength of 275 MPa.

Key words: *High strength steel; Fire resistance; concrete-filled steel tubular column; high temperature behaviour; numerical model.*

* Corresponding author. Tel.: +852-2859-2674; fax: +852-2559-5337.
E-mail address: young@hku.hk (B. Young).

1. Introduction

Concrete-filled steel tubular (CFST) columns have been widely used in the construction of framed structures in high-rise buildings due to their fine-looking appearance, high-bearing capacity and ductility, fast construction and cost-saving features. However, the main disadvantage of the CFST column is that the steel tube is exposed, thus leading to a lower fire resistance compared with concrete encased steel composite columns or even conventional reinforced concrete columns.

Experimental investigations were conducted on the behaviour of various concrete-filled steel tubular columns subjected to axial compressive forces in fire as detailed in Lie and Caron [1-3], Lie and Irwin [4], Chabot and Lie [5], Kodur and Lie [6], Han et al. [7], Lu et al. [8], Sakumoto et al. [9], Kordina and Klingsch [10], Chung et al. [11]. Extensive reviews on most of these research findings were done by Hong and Varma [12].

Although considerable work has been carried out in this area for concrete-filled hot-rolled mild steel tube columns, there is a lack of information for concrete-filled high strength steel tube columns in fire. High strength stainless steel with measured 0.2% proof strength of up to 536 MPa has been conducted by Young and Ellobody [13] for concrete-filled high strength stainless steel tube columns at normal room temperature (approximately 22℃). Up-to-date, there is still a lack of information for the fire resistance of CFST columns using high strength steel. Therefore, it is important to investigate the behaviour of concrete-filled high strength steel columns in fire. Due to the fact that experimental tests of CFST columns in fire are rather expensive, finite element analysis is one of the solutions to investigate the CFST columns. The fire resistance of hollow structural steel section columns filled with high strength concrete has been investigated numerically by Schaumann et al. [14].

The main objective of this study is to investigate the effects of high strength structural steel CFST columns under fire condition. Finite element model was initially developed to carry out both the numerical heat transfer analysis and nonlinear analysis using finite element program ABAQUS [15]. The finite element results were verified against experimental results of concrete-filled mild steel columns reported by the National Research Council of Canada (NRCC) [1, 3]. The comparison indicated that the finite element model was reasonably accurate for the simulation of CFST columns in fire. Based on the results obtained, an extensive parametric study was conducted to investigate the behaviour of concrete-filled normal and high strength steel circular columns under the ISO fire curve. The column time-temperature and time–axial shortening curves were evaluated.

2. Finite element modelling

2.1. General

In order to simulate the tests [1, 3] accurately, detailed information of the tests have been included in the finite element (FE) model. In the past, 2-D model was employed in thermal analysis to predict the temperature distribution [4, 16]. The total length of the columns in the tests was 3810 mm, although only the central part (around 3084 mm) was directly exposed to fire. The column temperature was uniform in the central heated part and dropped quickly to the room temperature outside the heated part, which led to a slightly longer fire failure time compared with uniform temperature assumption along the column. Besides, the thermal expansion of columns was affected by the heated length of columns. Therefore, the 3-D FE model only heated in central

part was used to simulate the temperature distribution characteristic, as shown in Fig.1. The end-plates of the columns were included in the FE model.

The analysis of structural fire resistance is a complicated process because it involves many variables such as: (1) fire growth and duration, (2) temperature distribution in structural elements, (3) initial imperfection of structural members, (4) interaction between structural components, (5) changes in material properties and the deformations, and (6) strength of the structures during exposure to the fire. In addition to these parameters, the choice of the element type and mesh size that provide accurate results with reasonable computational time is also important in simulating structures with interface elements.

2.2. Finite element mesh

To investigate the effect of different finite element meshes on thermal and structural analysis of the CFST columns in fire, a comparison of simulation results was conducted by using three different meshes. Column 4 (as detailed in Table 2) from NRCC [1, 3] was chosen for this analysis and the three different meshes are shown in Fig. 1 and Table 1. Mesh A and mesh B have the same mesh along their length, while mesh B and mesh C have the same cross-sectional mesh. Table 1 compares the predicted temperature of the centre of mid-span cross-section at 80 minutes and fire resistance of the CFST columns. The results from the comparison include: (1) the fire resistance increases with the finer mesh in cross-section and decreased with the finer mesh along the length direction of the column; (2) only tetrahedron-mesh in centre of section will not cause divergence. The relatively coarse mesh B in Fig. 1 is sufficient with high efficiency. Therefore, the mesh B has been used in all the thermal and structural analysis.

Different element types were examined in order to identify a suitable element to simulate the behaviour of the CFST column in fire. Solid elements were found to be more efficient in modelling the steel tube and the concrete as well as the clearly-defined boundaries of their elements. Three-dimensional eight-node solid element DC3D8 and C3D8 were used in the thermal and structural analysis, respectively.

2.3. Thermal analysis

A thermal 3-D finite element analysis was firstly performed for the CFST columns investigated in this study, using the heat transfer option available in ABAQUS [15]. A constant convective coefficient (α_c) of 25 W/m^{2}K was assumed for the exposed surface, and 9 W/m^{2}K was assumed for the unexposed surface. The radiative heat flux was calculated using a steel emissivity (e) value of 0.8 and the Stefan-Boltzmann constant (σ) was 5.67×10^{-8} W/m^{2}K^4. These governing parameters values were recommended in EC1 [17]. The specific heat and thermal conductivity of concrete was calculated according to EC2 [18] with the moisture content considered in the calculation of specific heat of concrete. The specific heat and thermal conductivity of steel was calculated according to EC3 [19]. The values of the thermal expansion coefficient ($\Delta l/l$) 12×10^{-6}/℃ and 6×10^{-6}/℃ for steel and concrete used by Hong and Varma [12] were employed, respectively. Heat flux continuity condition was assumed at the interface between the steel tube and concrete core.

2.4. Concrete-steel interface

According to the process of fabricating specimens [1, 3], the possible effects of the composite interaction between the steel and the concrete infill were investigated by considering two models: (1) full bond between the end-plate and the concrete, with the contact between the

steel tube and the concrete modelled by interface elements, by which the gap between the steel tube and concrete was assumed; (2) contact between the steel tube and the concrete, with contact between the end-plate and the concrete modelled by the interface elements, a slip between the steel tube and concrete was assumed.

The two models mentioned above were used to analyze the fire resistance of the CFST columns for Column 4 (as detailed in Table 2), while the mechanical properties of concrete and steel as specified in EC4 [20] were used at elevated temperatures. Fig. 2 shows that (a): the column fire resistance times were quite close for the column test and the predications by the two models since the ultimate failure mode of the CFST columns is the concrete core lost its strength at the certain temperatures, whereas no difference was noted in thermal analyses； (b) the shape of the time-axial displacement curves obtained by Model 2 showed a good agreement with the experimental results, which indicated that it would be impossible to simulate the performance of the CFST columns, when the steel tube resisted the applied load corresponds to larger thermal expansion, with the column suddenly contracted as the steel tube lost its load carrying capacity due to buckling of the steel tube. This was not surprising because the steel tube and concrete core would have been separated due to the different thermal expansions in both the longitudinal and radial directions when exposed to fire [16].

For the purpose of examining the effects of high strength structural steel on the fire resistance of CFST columns, Model 2 was selected to simulate the fire resistance of the CFST columns. It is not necessary to consider the bond stress of concrete-steel interface [16], because even in ambient, the bond stress of the plain steel and concrete interface is very small, and the tendency of the slip or the gap would be found as soon as the column is heated. The properties of contact model are recommended by Ellobody and Young [21].

2.5. Steel and concrete material properties

It is well known that the mechanical material properties at elevated temperatures significantly affect the fire resistance of CFST columns. The existing material models by Lei and Irwin's model [4], EC4 model [20] and Poh's steel model [22] were compared by previous researchers. However, different results were obtained despite the possible interaction between the steel tube and concrete was ignored. The three steel models were used to analyze the fire resistance of the CFST columns for Column 4 (as detailed in Table 2), while the EC4 model was used for concrete, and the results are shown in Fig. 3. The Lie and Irwin [4] and EC4 [20] concrete models were used to analyze the same specimen, while the EC4 model was also used for steel. The results are shown in Fig. 4. The comparison of the steel and concrete models for the time-displacement responses is shown in Figs 3 and 4.

The fire resistance calculated form EC4 steel model was the most conservative among the values obtained from the other material models, whereas the axial displacement with time was closest to the experimental data. The same conclusion could be drawn for the EC4 concrete model. Therefore, the EC4 [20] for concrete and steel models were selected for the finite element analysis. Moreover, the confinement for the concrete provided by the steel tube was not considered in the concrete stress-strain curve in this study. This is due to the thermal expansion of steel is larger than concrete.

2.6. Initial geometric imperfection and amplitude

An initial geometric imperfection was included in the finite element model to predict the overall buckling behaviour of the columns. Generally, the geometric imperfection for a member is specified as the first bucking mode shape multiplied by the magnitude. Since the actual column

specimens were not reported, three assumed values of imperfection were considered for the imperfection sensitivity analyses. Fig. 5 compares the axial displacement effects for Column 4. Larger imperfection magnitudes reduce the failure time of the CFST column. The initial geometric imperfection equal to L/1000, where L is the column length, gives most favourable comparisons between FE models and the test results, and the same result obtained by previous investigation as detailed in Ding and Wang [16]. This value of L/1000 was used in the verification and parametric studies.

3. Verification of finite element model

Using the FE model described in this paper, the axial displacement and the fire resistance were obtained for the six columns given in Table 2. These specimens were tested at the NRCC [1, 3]. In the column tests, the ambient temperature at the start of each test was approximately 20℃. During the test, the column was exposed to ASTM-E119 [23] standard temperature-time curve, which was lower than ISO-834 [24] fire curve. All the tested specimens were circular hollow sections, filled with siliceous aggregate concrete and subjected to concentric compression load.

The temperatures obtained from the FE model were compared with those measured at the external surface and at various depths of the steel tube sections for the six columns, as shown in Fig 6. It was obvious that there was reasonably good agreement between the FE and test results, especially at the external surface of the steel tubes. In the earlier stages of fire exposure, for locations deeper in the concrete, the temperature readings obtained by the FE model were higher than the measured temperatures, which kept nearly constant values after a rapid rise. This difference might be due to the result that migration of moisture towards the centre was not taken

into account in the FE model. At a later stage, when content of the moisture in concrete was almost zero, the temperatures predicted by the FE analysis were generally in good agreement with the test results.

The axial displacement obtained from the FE model and the measured axial displacement at the top of the columns are compared in Fig. 7 for the six columns. Despite there were some differences between the FE predictions and test results, the agreement of tendency was generally good. The predicted and measured positive maximum displacement values at the top of the columns were compared in Table 2. The FE predicted values were in good agreement with the experimental results, which confirmed that the coefficient of thermal expansion of steel and the concrete-steel interface of FE model used in this study worked well. In the time-axial displacement curves, the steel tubes softened with the increased temperatures and the columns suddenly contracted due to buckling of the steel tube, as shown in Fig. 7. Finally, the column resisted the heat until the concrete core collapsed. In general, the predicted displacement near the point of failure was smaller than the measured displacement. It is likely that the main cause of the difference related to the creep of the steel and concrete, which became more pronounced at higher temperatures. A part of the creep, however, was implicitly taken into account in describing the mechanical properties of the materials used [25].

The failure criterion provided by the BS-476 [26] gives two limits: the tests are usually stopped when certain limitation on deflection magnitude or deflection rate has been reached, e.g. $L/20$ and $(L^2)/(9000/D)$, where D is the diameter of the column. In this study, all the limited values of the rate of deflection according to BS-476 were adopted in the finite element analysis. In the FE model, the general failure time for the columns was defined as the point at which the column could no longer support the load. The time-axial displacement curves in Fig. 7, the open

dots stand for the failure time limited by the BS-476 [26]. It is found that the failure time between the BS-476 [26] and FE predictions are quite close, which showed that the failure criterion of BS-476 is reasonable. The measured and predicted fire resistances of the six columns are compared in Table 2. Generally, good agreement was achieved between the test results and the finite element results. The mean value of FE fire resistances to test fire resistance ratio is 1.05 with the corresponding coefficient of variation (COV) of 0.044, as shown in Table 2.

4. Parametric study and discussion

The objective of the parametric study is to investigate the effects of high strength structural steel on the fire resistance of CFST columns under constant axial load. For this purpose, the fire resistance of CFST columns using the high strength steel with nominal yield strength of 690 MPa was compared with those using normal strength steel with nominal yield strength of 275 MPa in the parametric study. The material properties of high strength steel at elevated temperatures were recommended by Chen and Young [27]. Furthermore, a stress-strain curve model of high strength steel for temperature ranged from 22 to 1000℃ has been proposed by Chen and Young [28]. This material model has been used for modelling the fire performance of high strength steel columns [28].

In this study, a total of 37 columns were analyzed using the verified finite element model in the parametric study, and the dimensions and material properties of columns are summarized in Table 3. The parametric study included different strength of steel and concrete, different cross-sectional dimensions, different load ratios, different types of aggregates and different moisture contents of concrete. The load ratio during fire is defined as the applied load divided by the

nominal strength (unfactored design strength) at ambient temperature calculated based on EC4 [29] varied from 0.24 to 0.54, as shown in Table 3.

The columns were divided into 5 groups (G1-G5). The two groups G1 and G3 columns had the same diameter of 400 mm, and the diameters of the columns in groups G2, G4, G5 were 200 mm. The steel strength of columns of the first two groups G1 and G2 had three levels: S275, S460 and S690, having the nominal yield strengths of 275, 460 and 690 MPa, respectively. The concrete cylinder compressive strength (f_{ck}) of columns of groups G1 and G2 were 30 MPa and 50MPa, roughly the same as the tests [3], which were chosen to be less than 60 MPa due to the significant differences between the testing and numerical results for high strength concrete-filled steel columns [14]. Each specimen having the same material properties had two different load ratios of 0.3 and 0.5, as shown in Table 3. These columns were filled with siliceous aggregates concrete, in which the fire resistance were shorter than those filled with carbonate aggregates concrete [3]. A high moisture content of 10% of the concrete weight was assumed in the analysis since the moisture can hardly escape due to the surrounding steel section.

Group G3 was identical to G1, except the load was constant as 2933 kN instead of two constantly the load ratios for each specimen having the same material properties. In Group G4, the material properties and applied load of S30, S31, S32 and S33 were identical to columns S13, S21, S16 and S24 respectively, except for having carbonate aggregates instead of siliceous aggregates. The values for the main parameters of the stress-strain relationships of normal weight concrete with carbonate aggregates concrete at elevated temperatures was also recommended in EC2 [18]. Finally in Group G5, columns S34 and S35 were identical to column S15, except the concrete having different moisture contents of 0% and 5% by weight instead of 10%, respectively. In the same way, columns S36 and S37 were based on column S23, and the moisture contents varied.

The CFST columns investigated in the parametric study had the same overall column length (L) of 4000 mm, which resulted in different slenderness ratios $\bar{\lambda}$ (calculated based on EC4) that varied from 0.16 to 0.47. It should be noted that the effective buckling length (L_e) is equal to kL, where k is the effective length factor which is equal to 0.5 for fixed-ended column. The columns in the parametric study were heated using the standard fire curve [24].

The positive maximum axial displacement ($\delta_{\max}$) during fire and the fire resistance at failure of the CFST columns obtained form the parametric study were summarized in Table 4. The time-axial displacement relationships were also plotted as shown in Figs. 8-11 and 16-18. Furthermore, two failure modes were predicted from the finite element analysis. Generally, the relative slenderness ratio of the column ($\bar{\lambda}$) affected the failure mode. In this parametric study, the diameter of the column could be used to reflect the relative slenderness ratio due to the constant value of the column length. The columns with a small diameter of 200 mm failed by flexural buckling (F), whereas the larger diameter of 400 mm failed by crushing of the concrete in compression (C), as shown in Table 4.

Fig.12 plotted the load ratio-fire resistance relationships for the CFST specimens of G1 and G2. The fire resistance of the columns obviously decreased with an increase in the column load ratio, especially for G1 that had a bigger diameter. Fig.13 and Fig.14 showed the effects of different strength of steel and concrete on the fire resistance of the column specimens of G1 and G2, respectively. Generally, it can be seen that at the same load ratio, the fire resistance is decreased with an increase in the strength of steel, while it increased with an increase in the strength of concrete. As to the reason for this shown in Figs. 8-11, the steel tube would lose its strength after 20 to 30 minutes of exposure to fire. From that time the concrete core would take

over the load that carried a progressively increasing portion of the load with a rising temperature. At the same load ratios, the higher the yield strength of steel, the more load would be transferred from the steel tube to concrete core. Fig. 15 plotted the concrete load intensity-fire resistance relationships for the CFST columns of G1 and G2 having the section diameters of 200mm and 400mm. As expected, the concrete load intensity (P/P_c) indicated an obvious relevance with the fire resistance of the CFST columns.

Fig. 16 compared the time-axial displacement relationships for G3 and S4 under the same load 2933 kN. It showed that under the same load, the maximum displacement of CFST with S690 steel was almost double as much as than that of CFST with S275, and the fire resistance time could be increased to around 20 minutes from S275 to S690. The fire resistance could be increased to around 80 minutes from C30 to C50, as shown in Fig. 16 and Table 5. The diameter and strength of concrete have a relatively larger influence than the strength of steel on the fire resistance time of CFST columns. Under the same load, the fire resistance of the CFST columns with the improved tube yield strength of 690 MPa had significant improvement than the steel tube of yield strength 275 MPa.

The effects of the aggregate type of concrete on the fire resistance of CFST column are shown in Fig. 17 for carbonate and siliceous aggregates concretes. Better performance can be expected by using carbonate aggregate. In the parametric study, the fire resistance for the column specimens S30, S31, S32 and S33 have 1.11, 1.07, 1.10 and 1.02 times than the corresponding specimens S13, S21, S16 and S24, for which the value of the concrete load intensities were 1.39, 2.85, 1.54 and 2.99, respectively. The added value of fire resistance using the carbonate aggregate compared with the siliceous aggregate increased with the decreased concrete load intensity. Special attention should be paid based on the EC2, which had no distinction in thermal properties

of different type of aggregates of concrete, and more added value of fire resistance would be expected, if the thermal character of an endothermic reaction that occurred in carbonate aggregate around 700℃ is considered [3]. Fig. 18 compared the time-axial displacement relationships for the G5, S15 and S23 having different moisture content. As expected, the fire resistance of CFST columns would be increased with the increased moisture content (u).

5. Conclusions

Based on the numerical investigation, the following conclusions could be drawn:

1. A 3-D finite element model on the fire resistance of concrete-filled high strength steel tubular columns has been developed and verified against test results.
2. It is important to consider the contact between the steel tube and the concrete core, and the contact between the column end-plates and the concrete in the finite element model. This is due to the different thermal expansions in steel and concrete, and the concrete would have been separated from the steel tube and column end-plates when exposed to fire in concrete-filled steel tubular (CFST) columns.
3. The comparison of the fire resistance and axial displacement of CFST columns using three different material models has showed that the EC4 model is slightly better than the other two material models.
4. The column diameter and strength of concrete had a relatively larger influence than the strength of steel on the fire resistance time of CFST columns. At the same load ratio, the fire resistance is decreased with an increase in the strength of steel, while it increased with an increase in the strength of concrete.

5. Under the same load, the fire resistance of the CFST columns with the improved tube yield strength of 690 MPa had significant improvement than the steel tube of yield strength 275 MPa.
6. It is found that better performance in the CFST columns by using carbonate aggregate compared to siliceous aggregate.

Acknowledgements

The authors are thankful to Prof. Ran Feng for providing valuable comments to the paper. The research work described in this paper was supported by a grant from the Research Grants Council of the Hong Kong Special Administrative Region, China (Project No. HKU719308E).

Nomenclature

B Buckling failure mode;

C Compression failure mode;

COV Coefficient of variation;

D Diameter of the column;

e Emissivity value.

FE Finite element;

f_{ck} The cylinder compressive strength of concrete;

f_y Yield stress of steel;

k Effective length factor;

L Length of column;

L_e Effective length of column;

P Load value;

P_c Sectional capacity of concrete core;

P/P_c Concrete load intensity;

r Global r-polar coordinate;

t Plate thickness of steel tube;

u Moisture content of concrete;

Z Global Z-polar coordinate;

α_c Convective coefficient;

$\delta_{\max}$ Maximum axial displacement predicted from finite element analysis;

θ Global θ-polar coordinate;

$\bar{\lambda}$ Relative slenderness ratio;

σ Stefan-Boltzmann constant;

$\Delta l / l$ Thermal expansion.

References

[1] Lie TT, Caron SE. Fire resistance of circular hollow steel columns filled with siliceous aggregate concrete. Test results, internal report no.570. Ottawa (Canada): Institute for Research in Construction, National Research Council of Canada (NRCC); 1988.

[2] Lie TT, Caron SE. Fire resistance of circular hollow steel columns filled with carbonate aggregate concrete. Test results, internal report no.573. Ottawa (Canada): Institute for Research in Construction, National Research Council of Canada (NRCC); 1988.

[3] Lie TT, Caron SE. Experimental studies on the fire resistance of hollow steel columns filled with plain concrete. Test results, internal report no.611. Ottawa (Canada): Institute for Research in Construction, National Research Council of Canada (NRCC); 1992.

[4] Lie TT, Irwin RJ. Fire resistance of rectangular steel columns filled with bar-reinforced concrete. Journal of Structural Engineering 1995; 121(5): 797–805.

[5] Chabot MM, Lie TT. Experimental studies on the fire resistance of hollow steel columns filled with bar-reinforced concrete. IRC internal report no.628. Ottawa (Canada): Institute for Research in Construction, National Research Council of Canada (NRCC); 1992.

[6] Kodur VK, Lie TT. Fire resistance of circular steel columns filled with fiber-reinforced concrete. Journal of Structural Engineering 1996; 122(7): 776–82.

[7] Han LH, Yang YF, Xu L. An experimental study and calculation of the fire resistance of concrete filled SHS and RHS columns. Journal of Constructional Steel Research 2002; 59: 427–52.

[8] Lu H, Zhao XL, Han LH. Fire behaviour of high strength self-consolidating concrete filled steel tubular stub columns. Journal of Constructional Steel Research 2009; 65(10-11): 1995–2010

[9] Sakumoto Y, Okada T, Yoshida M, Taska S. Fire resistance of concrete-filled, fire-resistant steel-tube columns. Journal of Materials in Civil Engineering 1994; 6(2): 169–84.

[10] Kordina K, Klingsch W. Fire resistance of composite columns of concrete filled hollow sections. Research report. CIDECT 15 C1/C2–83/27. Germany. 1983.

[11] Chung K, Park S, Choi S. Material effect for predicting the fire resistance of concrete-filled square steel tube column under constant axial load. Journal of Constructional Steel Research 2008; 64: 1505–15.

[12] Hong Sangdo, Varma Amit H. Analytical modeling of the standard fire behavior of loaded CFT columns. Journal of Constructional Steel Research 2009; 65(1): 54–69.

[13] Young B, Ellobody E. Experimental investigation of concrete-filled cold-formed high strength stainless steel tube columns. Journal of Constructional Steel Research 2006; 62(5): 484–92.

[14] Peter Schaumann, Venkatesh Kodur, Oliver Bahr. Fire behaviour of hollow structural section steel columns filled with high strength concrete. Journal of Constructional Steel Research 2009; 65(8-9): 1794-802.

[15] ABAQUS. ABAQUS/standard version 6.6 user's manuals: Volumes I–III. Pawtucket (Rhode Island): Hibbitt, Karlsson, and Sorenson, Inc.; 2005.

[16] Ding J. and Wang Y.C, Realistic modelling of thermal and structural behaviour of unprotected concrete filled tubular columns in fire, Journal of Constructional Steel Research, 2008; 64(10): 1086-102.

[17] CEN (European Committee for Standardisation). EN 1991-1-2, Eurocode 1: Actions on structures, Part 1.2: General actions—actions on structures exposed to fire. London: British Standards Institution; 2002.

[18] CEN (European Committee for Standardisation). EN 1992-1-2, Eurocode 2: Design of concrete structures, part 1.2: General rules—Structural fire design. Brussels: CEN; 2004.

[19] CEN (European Committee for Standardisation). EN 1993-1-2, Eurocode 3: Design of steel structures, part 1.2: General rules—Structural fire design. Brussels: CEN; 2005.

[20] CEN (European Committee for Standardisation). EN 1994-1-2, Eurocode 4: Design of composite steel and concrete structures, part 1.2: General rules—structural fire design. London: British Standards Institution; 2005.

[21] Ellobody, E. and Young, B. Behaviour of normal and high strength concrete-filled compact steel tube circular stub columns. Journal of Constructional Steel Research, 2006; 62(7):706-15.

[22] Poh KW. Stress-strain-temperature relationships for structural steel. Journal of Materials in Civil Engineering 2001; 13(5): 371-9.

[23] ASTM. Standard test methods for fire tests of building construction and materials, E119. W. Conshohocken (PA): American Society for Testing and Materials; 2003.

[24] ISO-834. Fire resistance tests-elements of building construction. International Standards ISO 834. Geneva, Switzerland; 1975.

[25] Lie, T.T. and Chabot, M., Method to predict the fire resistance of circular concrete filled hollow steel columns, Journal of Fire Protection Engineering,1990; 2(4): 111-28.

[26] BS-476. Fire tests on building materials and structures. Method for determination of the fire resistance of elements of construction (general principles); 1987.

[27] Chen J, Young B. Experimental investigation of cold-formed steel material at elevated temperatures. Thin-Walled Structures 2007; 45(1): 96–110.

[28] Chen J, Young B. Design of high strength steel columns at elevated temperatures. Journal of Constructional Steel Research, 2008; 64(6): 689-703.

[29] CEN (European Committee for Standardisation). EN 1994-1-1, Eurocode 4: Design of composite steel and concrete structures, part 1.1: General rules and rules for building. London: British Standards Institution; 2004.

Mesh type	A	B	C
Mesh size of r direction (mm)	0.1	Min=0.072 Max=0.196	Min=0.072 Max=0.196
Mesh size of θ direction (mm)	0.1	0.2	0.1
Mesh size of z direction (mm)	0.3	0.3	0.5
Number of nodes	138153	54838	32902
Number of elements	91792	41476	24885
Temperature of the centre of concrete at 80 min (℃)	380.2	376.6	376.6
Fire resistance (minutes)	86.6	84.9	87.1

Table 1. Temperature and fire resistance comparison of different mesh

Column	Diameter	Wall Thick	Yield Strength	Concrete Strength	Test Load	Capacity of concrete	Concrete load intensity	The maximum displacement			Fire resistance		
	D (mm)	t (mm)	f_y (MPa)	f_{ck} (MPa)	P (kN)	P_c (kN)	$\frac{P}{Pc}$	$Test$ (mm)	FE (mm)	$\frac{FE}{Test}$	$Test$ (min)	FE (min)	$\frac{FE}{Test}$
1	141.3	6.55	401.93	31	131	100	1.31	24.09	21.72	0.90	57	58	1.02
2	219.1	4.78	322.06	32.3	492	278	1.77	18.13	15.68	0.86	80	87	1.09
3	219.1	4.78	322.06	32.3	384	278	1.38	18.77	17.50	0.93	102	111	1.09
4	219.1	8.18	367.43	31.7	525	256	2.05	20.36	18.69	0.92	82	85	1.04
5	273.1	5.56	412.79	27.2	1000	366	2.73	5.51	10.19	1.85	70	68	0.97
6	355.6	12.7	387.87	25.4	1050	543	1.93	22.51	18.36	0.82	170	182	1.07
									Mean	1.05		Mean	1.05
									COV	0.378		COV	0.044

Table 2. Comparison of test and finite element results

Group	Specimen	Section		Steel	Concrete			Load	Load
		D	t	f_y	f_{ck}	type of	Moisture	P	
		(mm)	(mm)	(MPa)	(MPa)	aggregate	(%)	(kN)	ratio
G1	S1	400	13.33	275	30	siliceous	10	1,622	0.30
	S2	400	13.33	275	30	siliceous	10	2,703	0.50
	S3	400	13.33	275	50	siliceous	10	1,760	0.30
	S4	400	13.33	275	50	siliceous	10	2,933	0.50
	S5	400	13.33	460	30	siliceous	10	2,516	0.30
	S6	400	13.33	460	30	siliceous	10	4,193	0.50
	S7	400	13.33	460	50	siliceous	10	2,651	0.30
	S8	400	13.33	460	50	siliceous	10	4,419	0.50
	S9	400	13.33	690	30	siliceous	10	3,590	0.30
	S10	400	13.33	690	30	siliceous	10	5,983	0.50
	S11	400	13.33	690	50	siliceous	10	3,724	0.30
	S12	400	13.33	690	50	siliceous	10	6,206	0.50
G2	S13	200	5.00	275	30	siliceous	10	295	0.30
	S14	200	5.00	275	30	siliceous	10	492	0.50
	S15	200	5.00	275	50	siliceous	10	327	0.30
	S16	200	5.00	275	50	siliceous	10	545	0.50
	S17	200	5.00	460	30	siliceous	10	440	0.30
	S18	200	5.00	460	30	siliceous	10	733	0.50
	S19	200	5.00	460	50	siliceous	10	471	0.30
	S20	200	5.00	460	50	siliceous	10	784	0.50
	S21	200	5.00	690	30	siliceous	10	606	0.30
	S22	200	5.00	690	30	siliceous	10	1,009	0.50
	S23	200	5.00	690	50	siliceous	10	635	0.30
	S24	200	5.00	690	50	siliceous	10	1,059	0.50
G3	S25	400	13.33	275	30	siliceous	10	2,933	0.54
	S26	400	13.33	460	30	siliceous	10	2,933	0.35
	S27	400	13.33	690	30	siliceous	10	2,933	0.24
	S28	400	13.33	460	50	siliceous	10	2,933	0.33
	S29	400	13.33	690	50	siliceous	10	2,933	0.24
G4	S30	200	5.00	275	30	carbonate	10	295	0.30
	S31	200	5.00	690	30	carbonate	10	606	0.30
	S32	200	5.00	275	50	carbonate	10	545	0.50
	S33	200	5.00	690	50	carbonate	10	1,059	0.50
G5	S34	200	5.00	275	50	siliceous	0	327	0.30
	S35	200	5.00	275	50	siliceous	5	327	0.30
	S36	200	5.00	690	50	siliceous	0	635	0.30
	S37	200	5.00	690	50	siliceous	5	635	0.30

Table 3. Specimen dimensions and material properties of CFST columns in the parametric study

Group	Specimen	$\bar{\lambda}$	Load P (kN)	Concrete capacity P_c (kN)	Concrete load intensity $\frac{P}{Pc}$	FE Failure mode	FE Fire resistance (min)	FE δ_{max} (mm)
G1	S1	0.16	1,622	821	1.98	C	151.2	23.15
	S2	0.16	2,703	821	3.29	C	53.7	15.92
	S3	0.17	1,760	1,368	1.29	C	226.7	21.89
	S4	0.17	2,933	1,368	2.14	C	128.5	12.27
	S5	0.20	2,516	821	3.07	C	73.5	21.38
	S6	0.20	4,193	821	5.11	C	32.8	16.27
	S7	0.21	2,651	1,368	1.94	C	154.3	20.99
	S8	0.21	4,419	1,368	3.23	C	56.3	14.24
	S9	0.25	3,590	821	4.37	C	46.3	23.22
	S10	0.25	5,983	821	7.29	C	31.5	17.14
	S11	0.25	3,724	1,368	2.72	C	90.0	22.34
	S12	0.25	6,206	1,368	4.54	C	38.0	15.65
G2	S13	0.31	295	213	1.39	F	58.5	23.36
	S14	0.31	492	213	2.32	F	36.7	16.29
	S15	0.32	327	354	0.92	F	73.3	22.38
	S16	0.32	545	354	1.54	F	51.0	13.74
	S17	0.39	440	213	2.07	F	43.0	21.88
	S18	0.39	733	213	3.45	F	27.5	17.65
	S19	0.40	471	354	1.33	F	58.8	21.04
	S20	0.40	784	354	2.21	F	36.8	15.37
	S21	0.47	606	213	2.85	F	33.5	23.99
	S22	0.47	1,009	213	4.75	F	23.3	23.30
	S23	0.47	635	354	1.79	F	50.5	23.04
	S24	0.47	1,059	354	2.99	F	25.8	18.15
G3	S25	0.16	2,933	821	3.57	C	42.4	13.31
	S26	0.20	2,933	821	3.57	C	53.6	20.73
	S27	0.24	2,933	821	3.57	C	63.9	25.13
	S28	0.21	2,933	1,368	2.14	C	134.8	20.01
	S29	0.25	2,933	1,368	2.14	C	152.4	24.72
G4	S30	0.31	295	213	1.39	F	65.2	22.34
	S31	0.47	606	213	2.85	F	36.0	23.99
	S32	0.32	545	354	1.54	F	56.1	16.71
	S33	0.47	1,059	354	2.99	F	26.3	13.74
G5	S34	0.32	327	354	0.92	F	56.6	22.43
	S35	0.32	327	354	0.92	F	63.7	22.40
	S36	0.47	635	354	1.79	F	38.2	23.05
	S37	0.47	635	354	1.79	F	43.9	23.06

Table 4. Results of failure mode, the maximum axial displacement and fire resistance of CFST columns in the parametric study

	Specimen	δ_{max} (mm)	Fire resistance (min)
Concrete	S4-S25	-1.04	86.1
	S28-S26	-0.72	81.2
	S29-S27	-0.41	88.5
Steel	S26-S25	7.42	11.2
	S27-S25	11.82	21.5
	S28-S4	7.74	6.3
	S29-S4	12.45	23.9

Table 5. Comparison of the maximum axial displacement and fire resistance of G4 and S4 having different strength of concrete and steel at the load 2933 kN

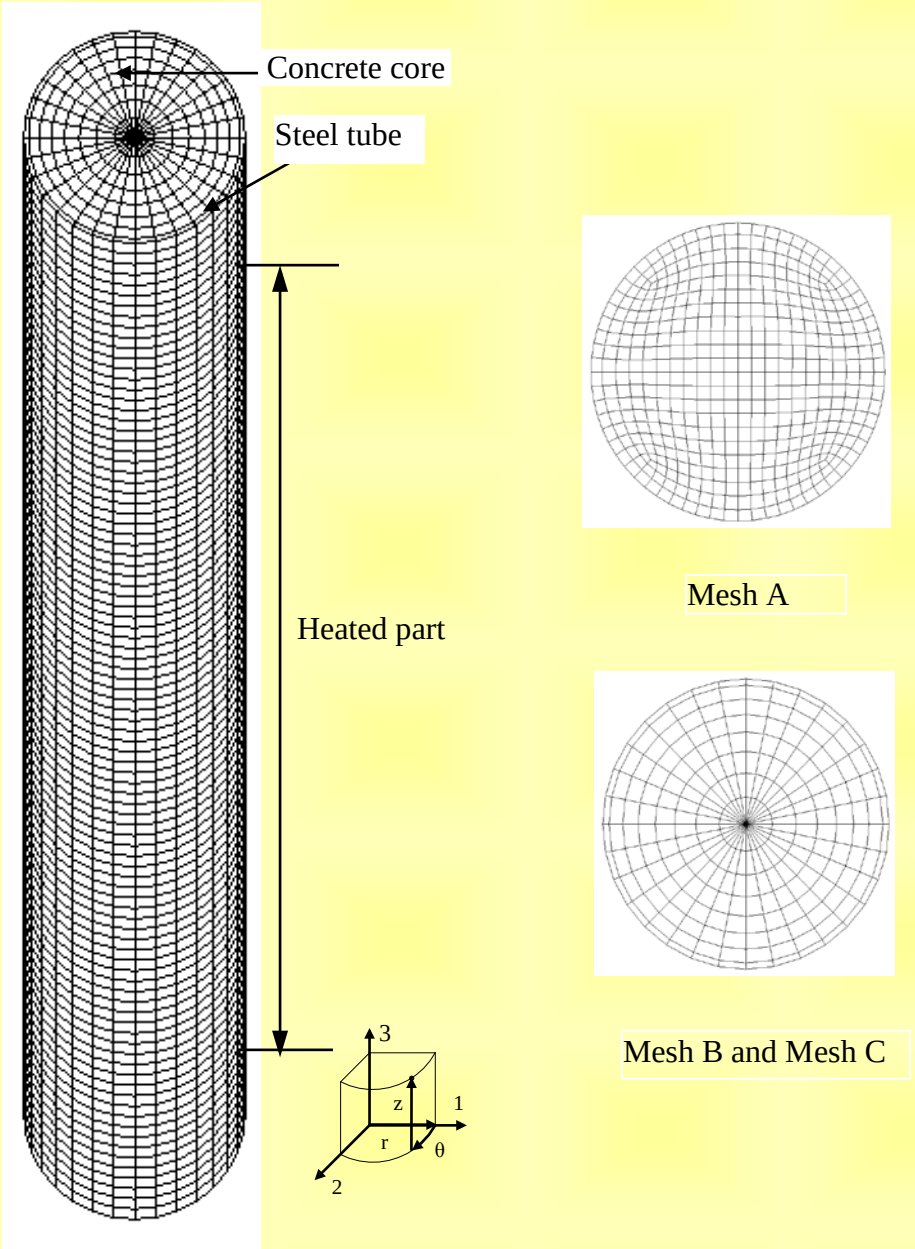

Fig. 1. Finite element model of CFST columns and effects of mesh size

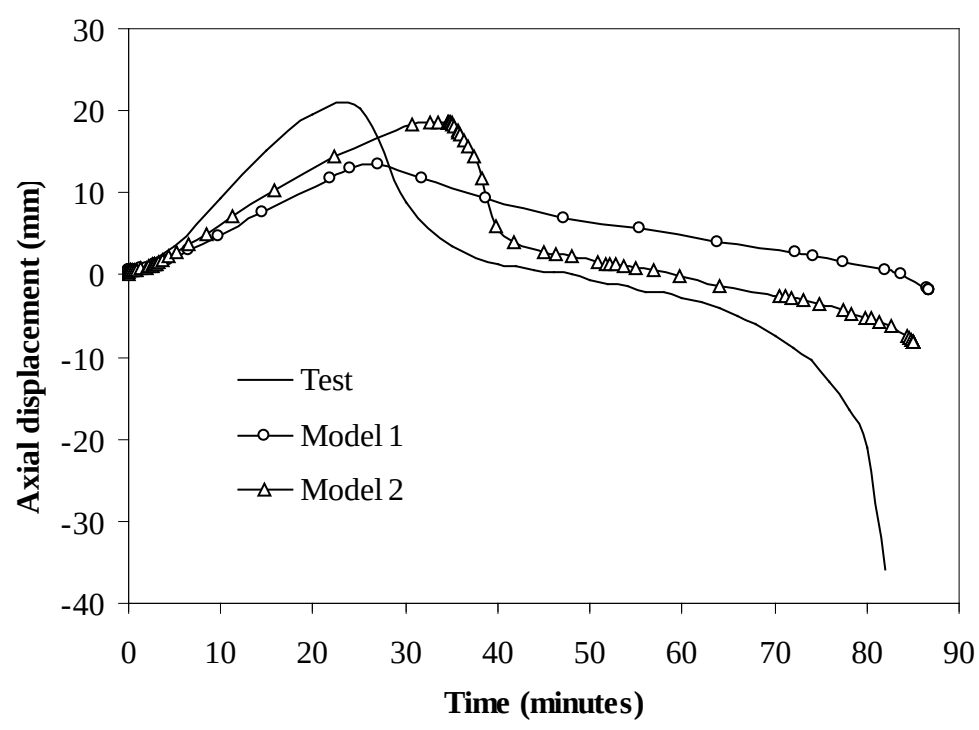

Fig. 2. Comparison of Time-axial displacement relationship with different concrete-steel interface models for column 4

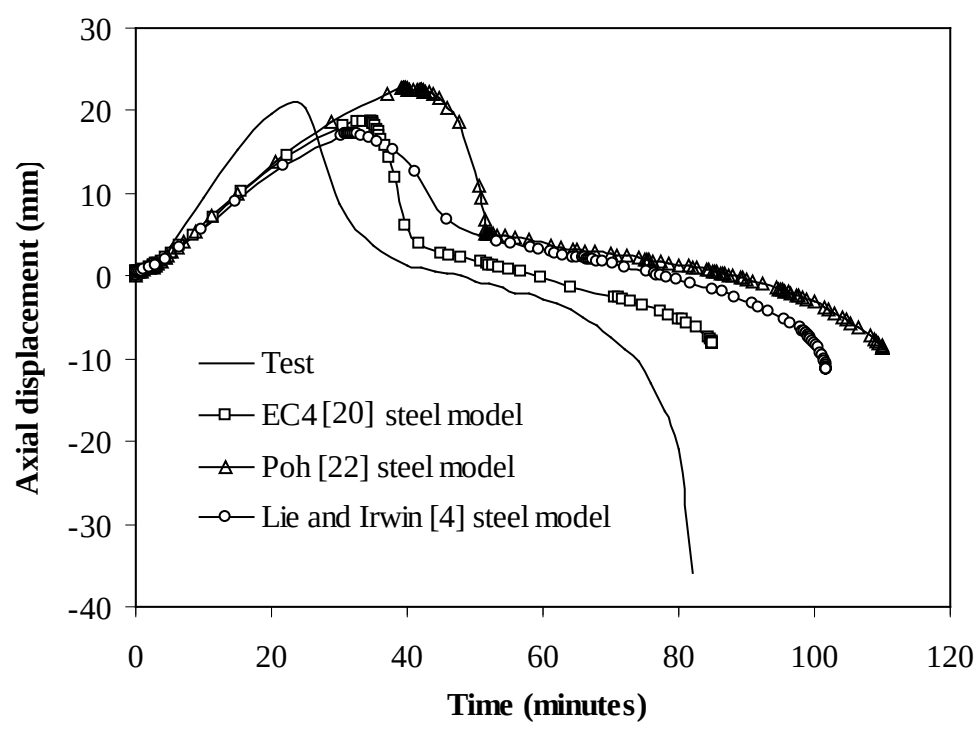

Fig. 3 Comparison of Time-axial displacement relationship with different steel models for column 4

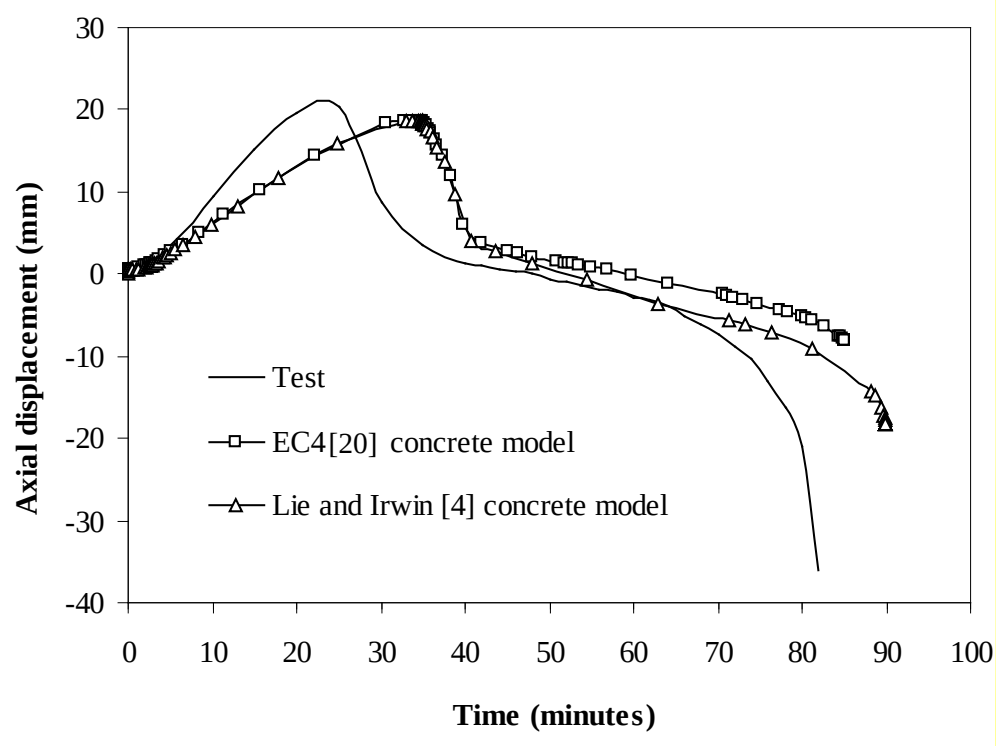

Fig. 4. Comparison of Time-axial displacement relationship with different concrete models for column 4

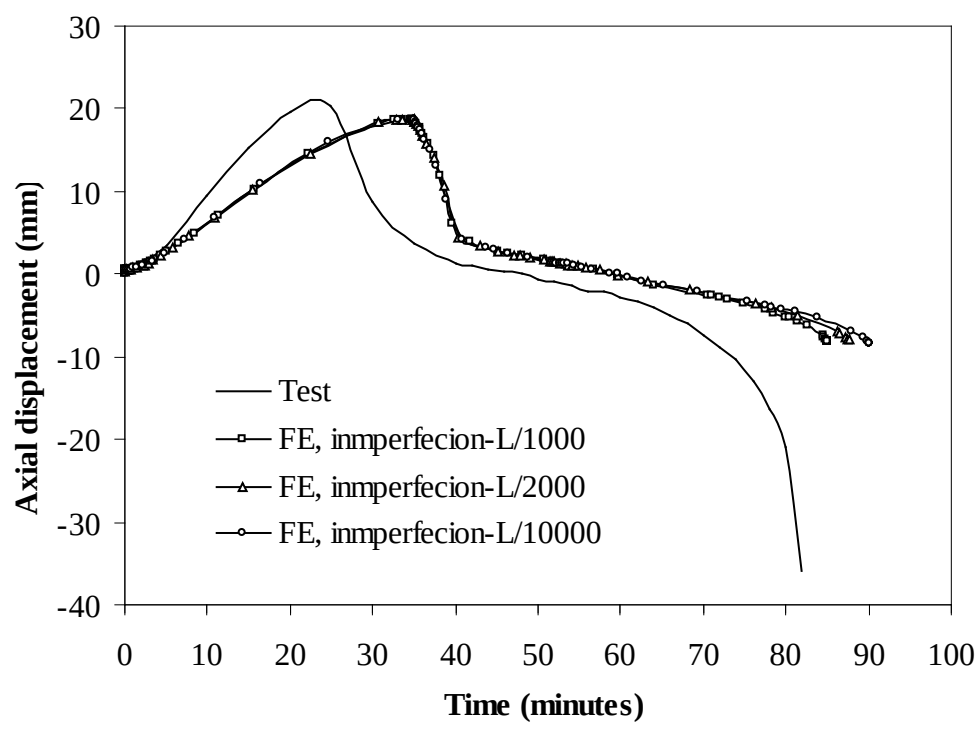

Fig. 5. Comparison of Time-axial displacement relationship with different initial geometric imperfections for column 4

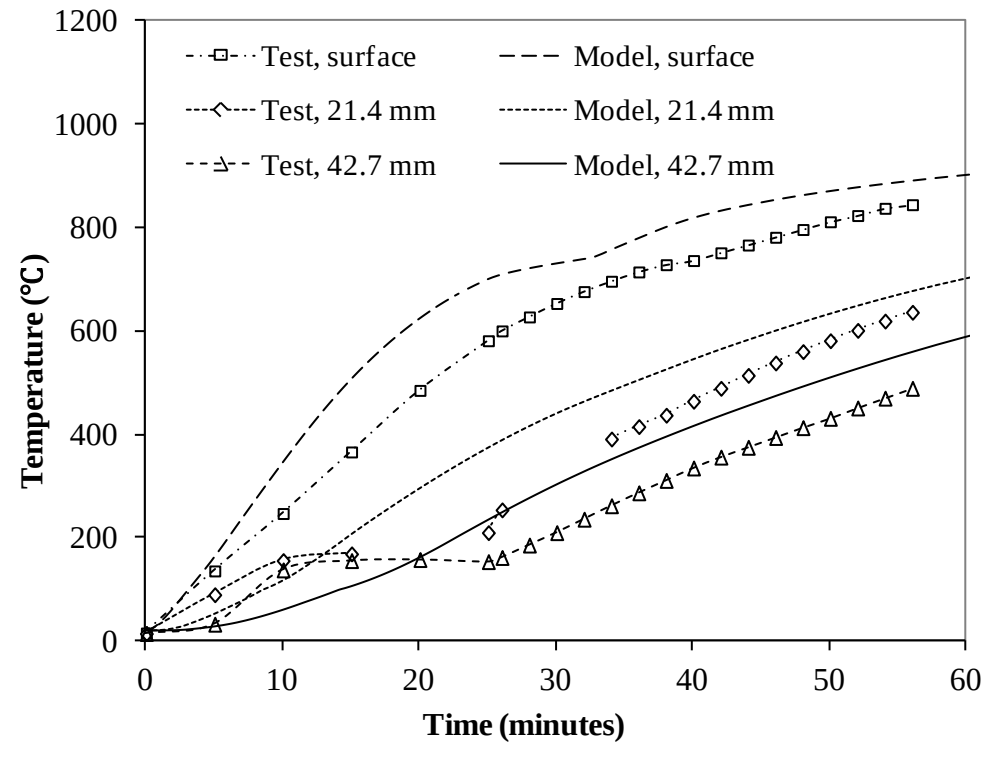

(a) Column 1

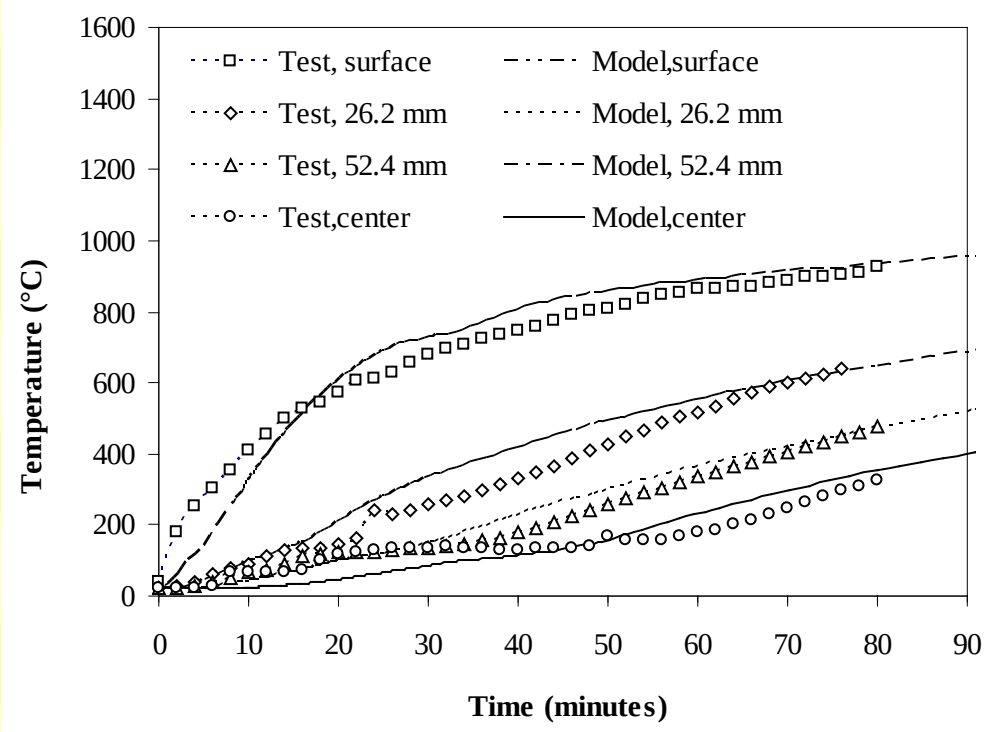

(b) Column 2

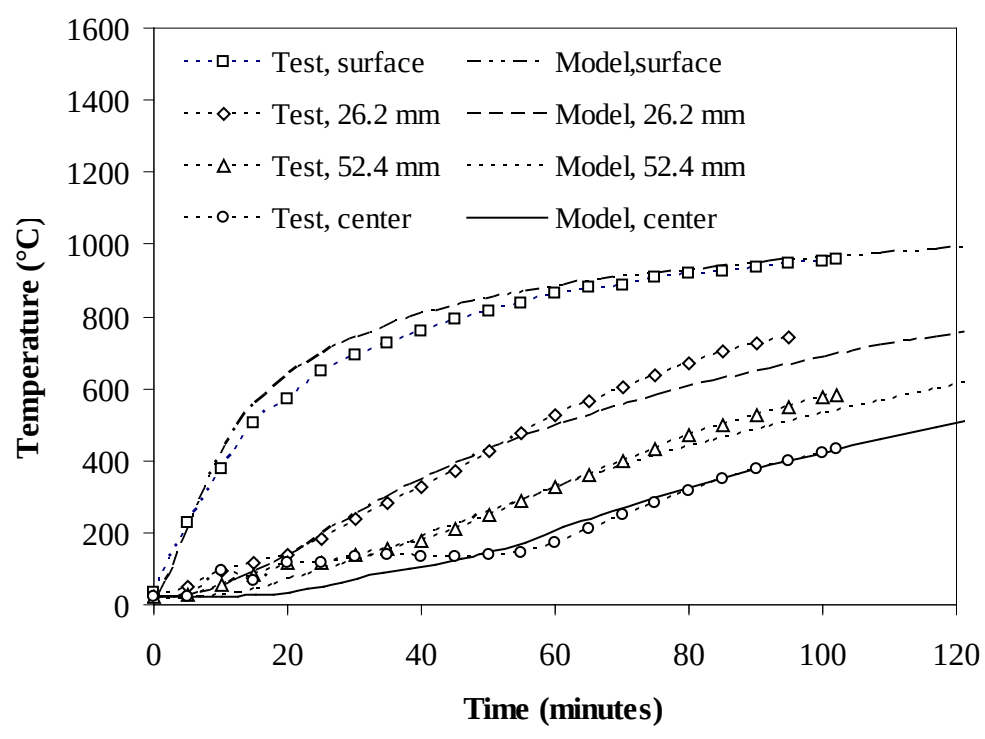

(c) Column 3

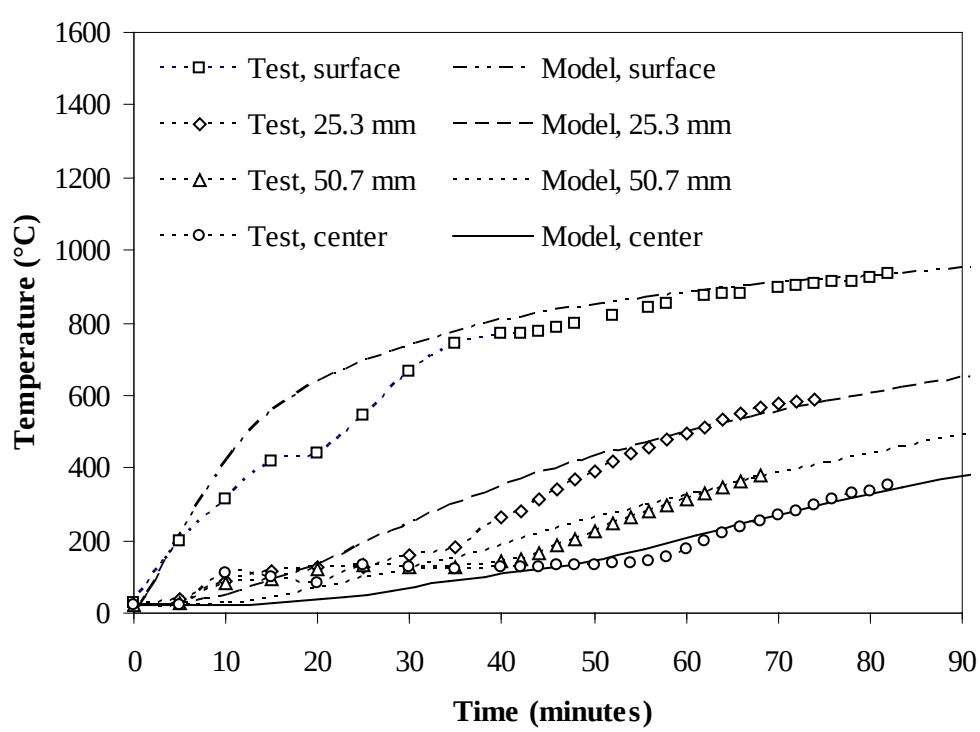

(d) Column 4

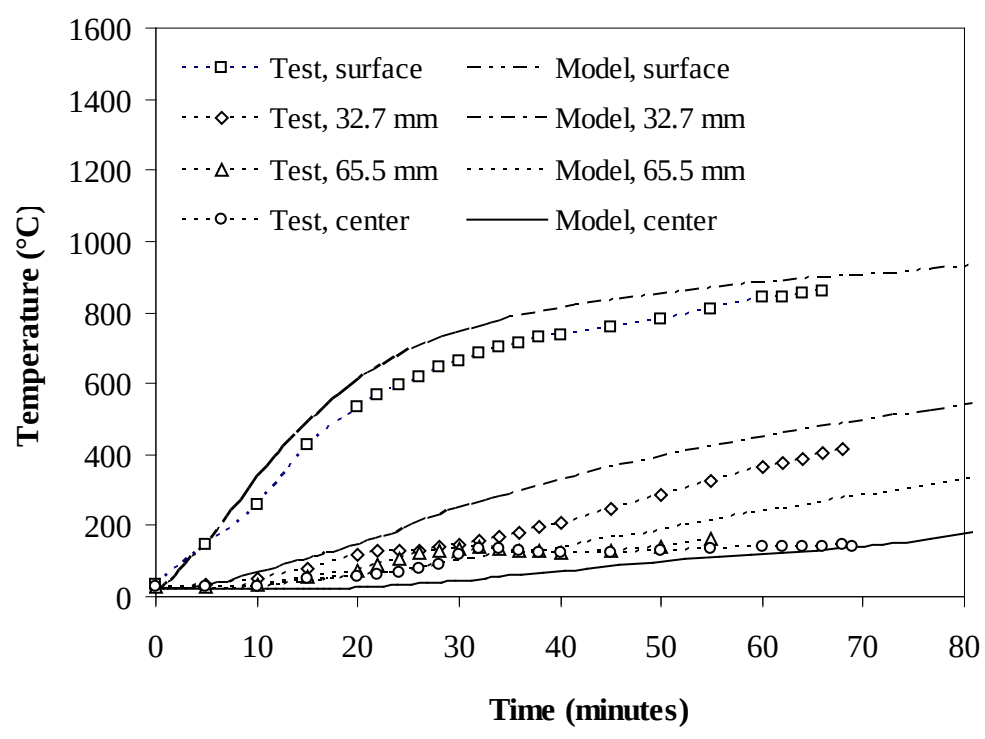

(e) Column 5

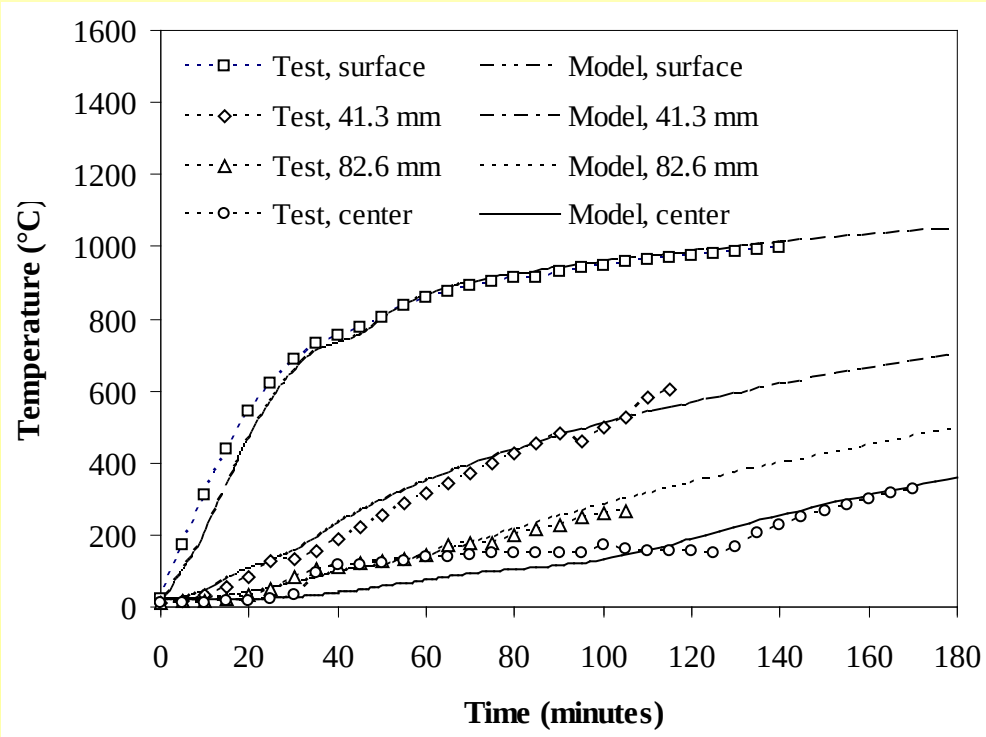

(f) Column 6

Fig. 6. Time-temperature relationships obtained experimentally and numerically for Columns 1-6

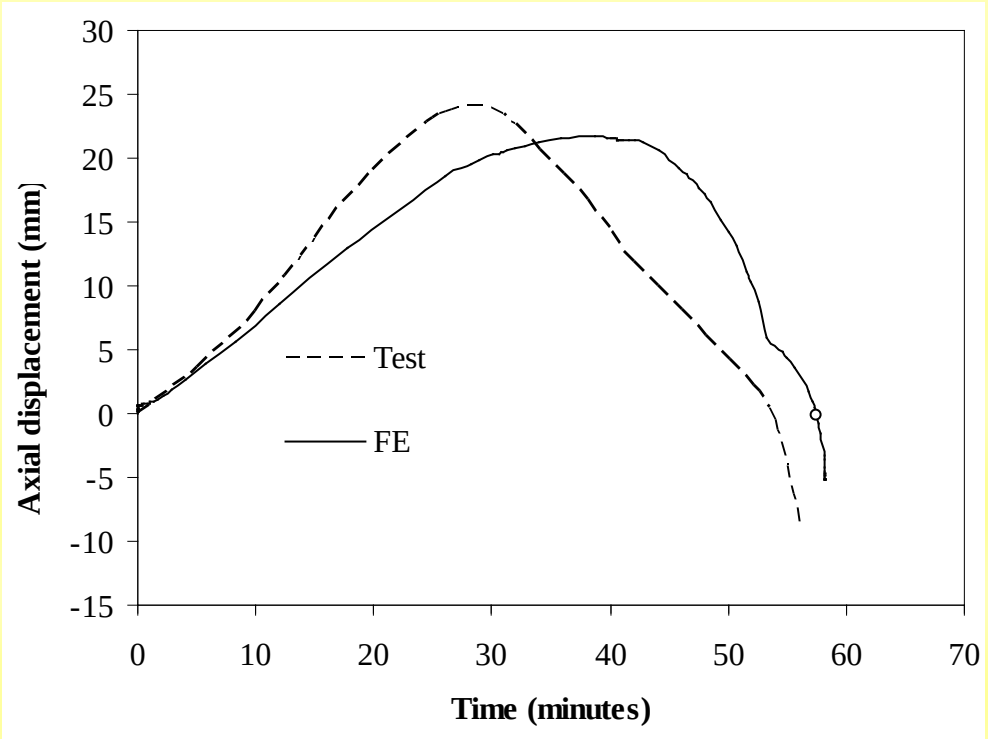

(a) Column 1

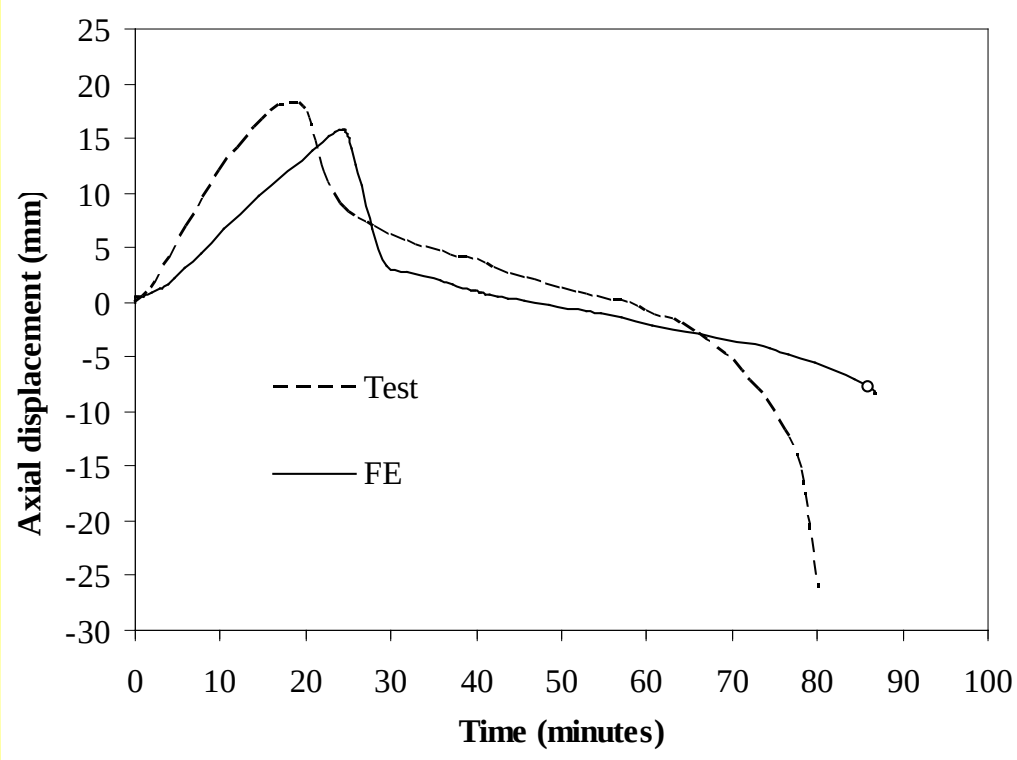

(b) Column 2

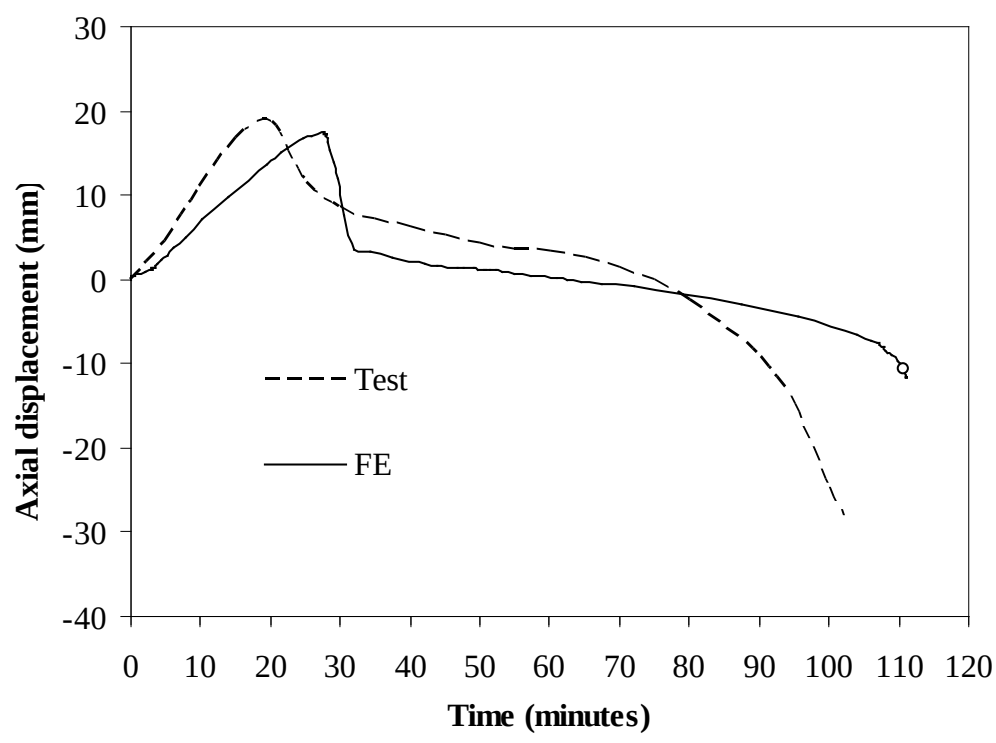

(c) Column 3

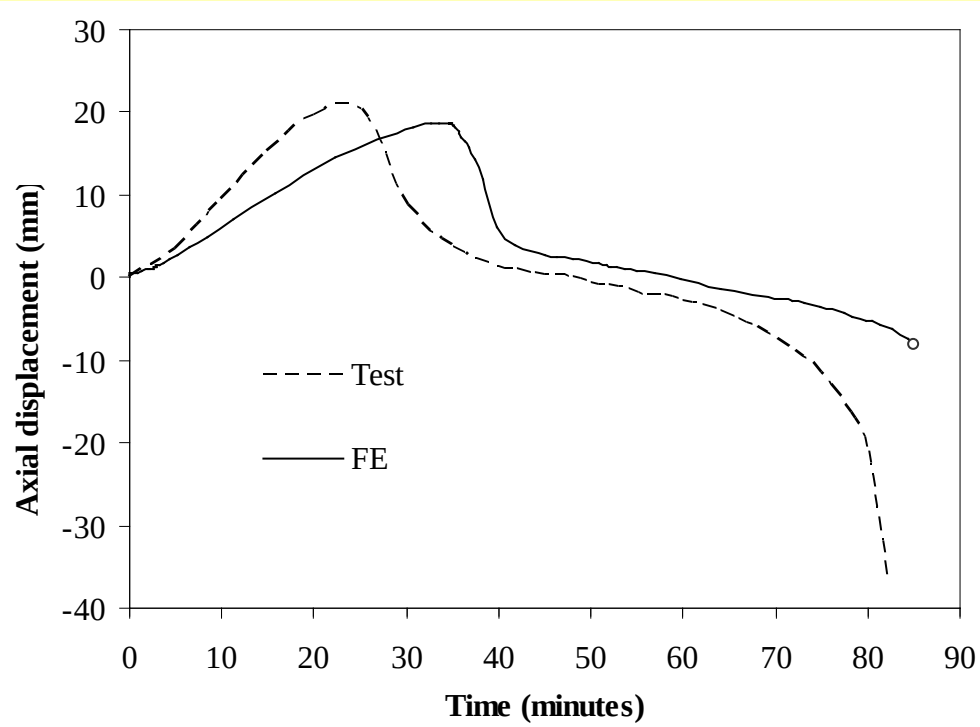

(d) Column 4

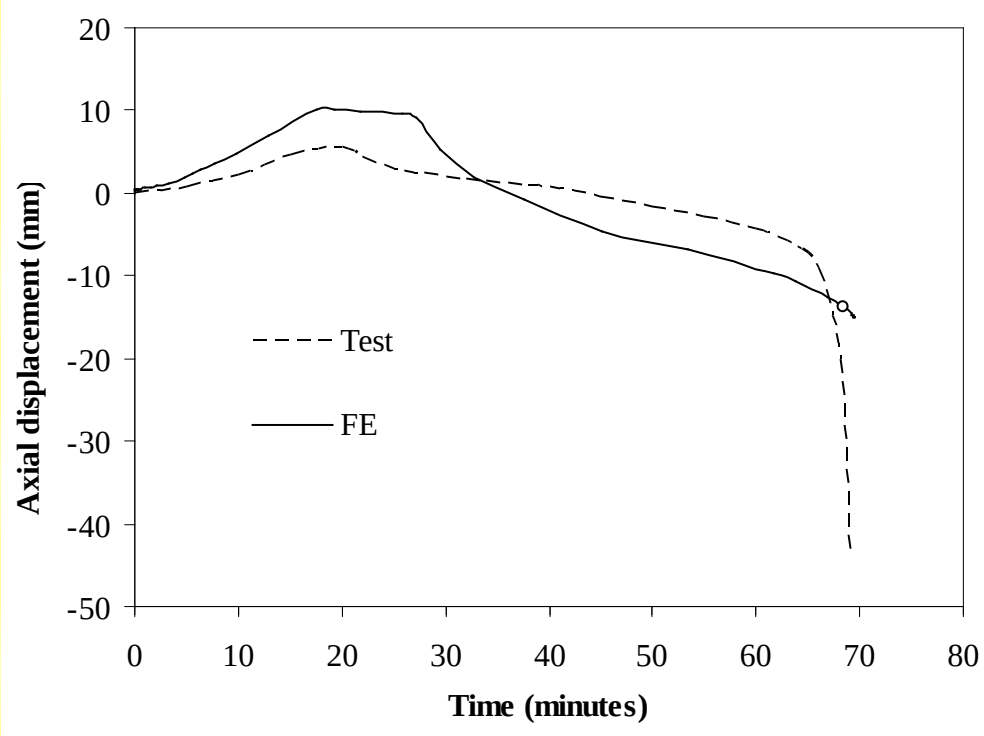

(e) Column 5

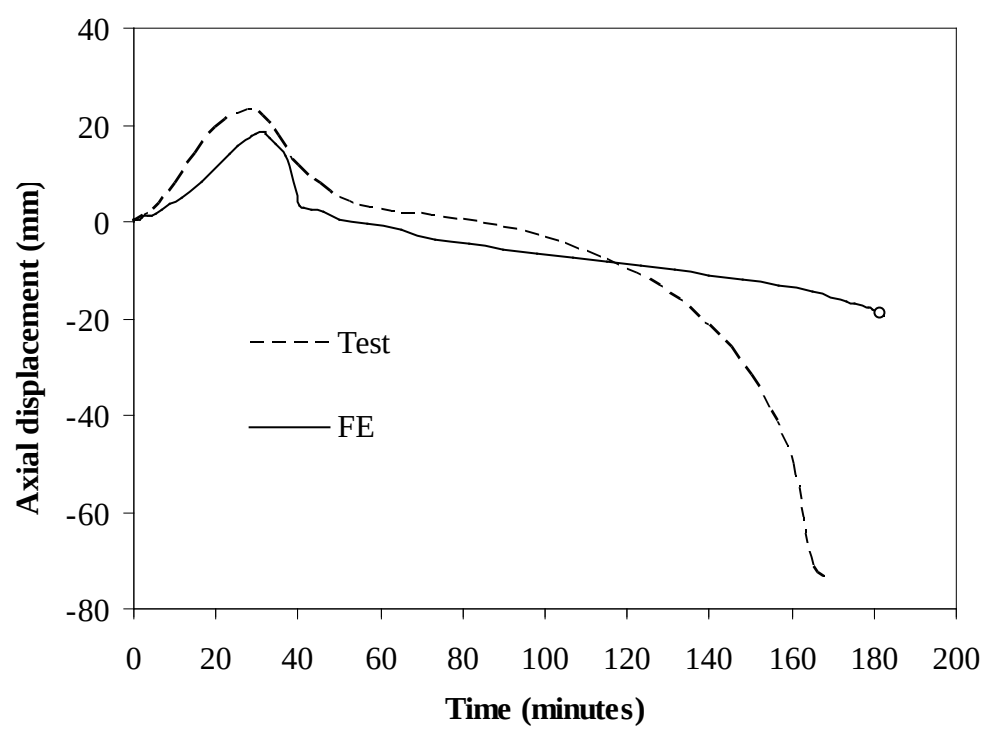

(f) Column 6

Fig. 7. Time-axial displacement relationships obtained experimentally and numerically for Columns 1-6

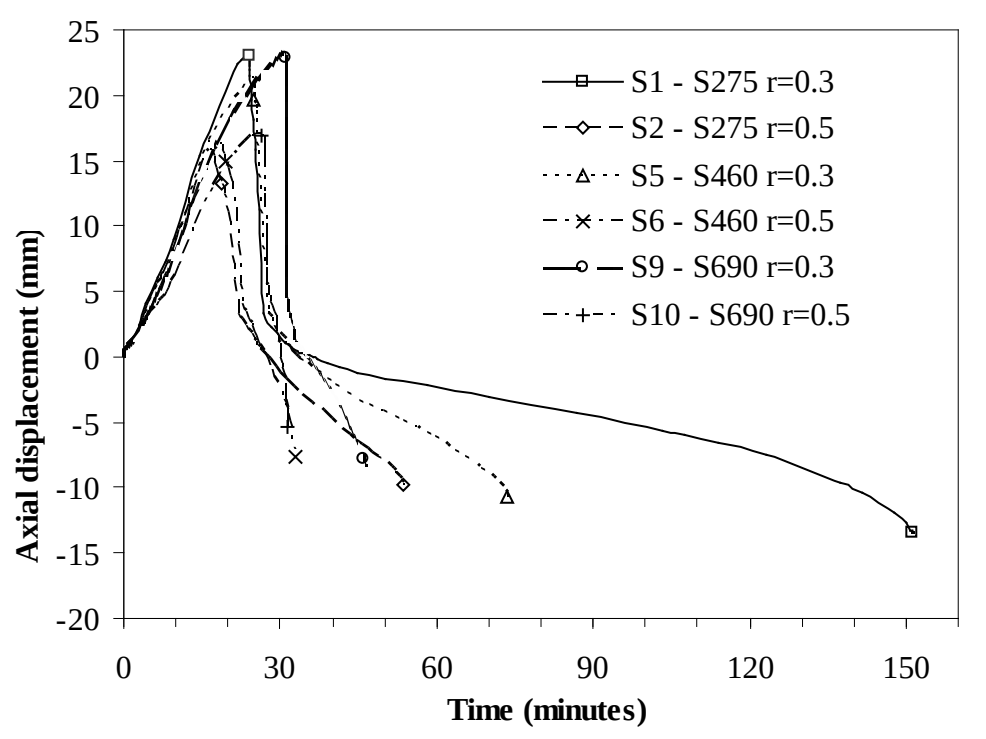

Fig. 8. Time-axial displacement relationships for S1, S2, S5, S6, S9 and S10

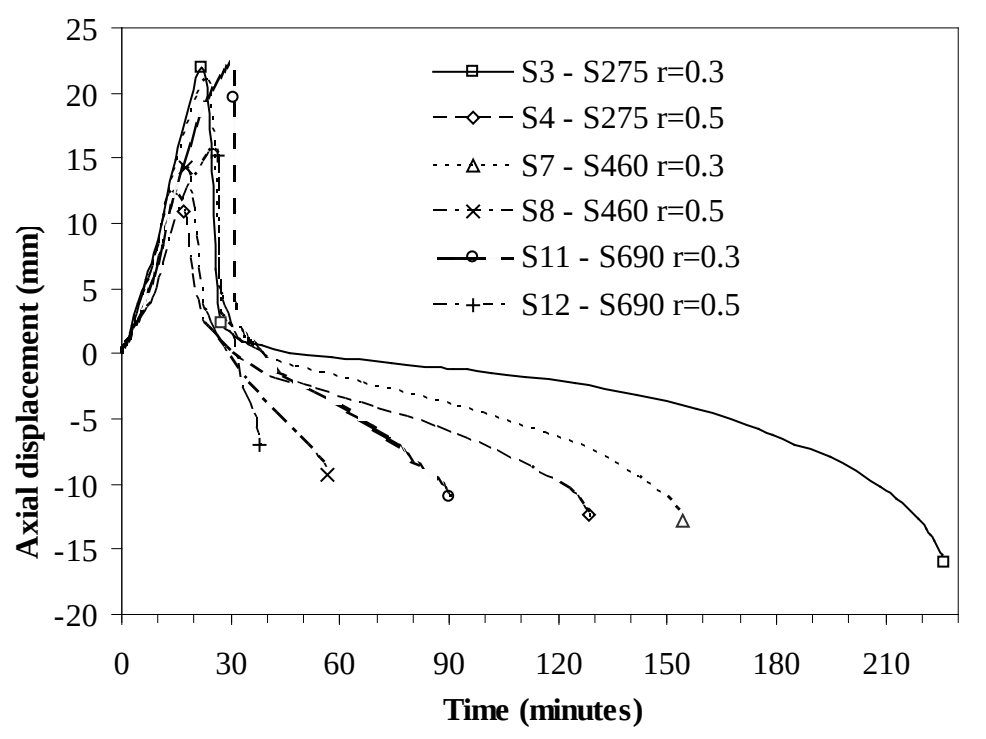

Fig. 9. Time-axial displacement relationships for S3, S4, S7, S8, S11 and S12

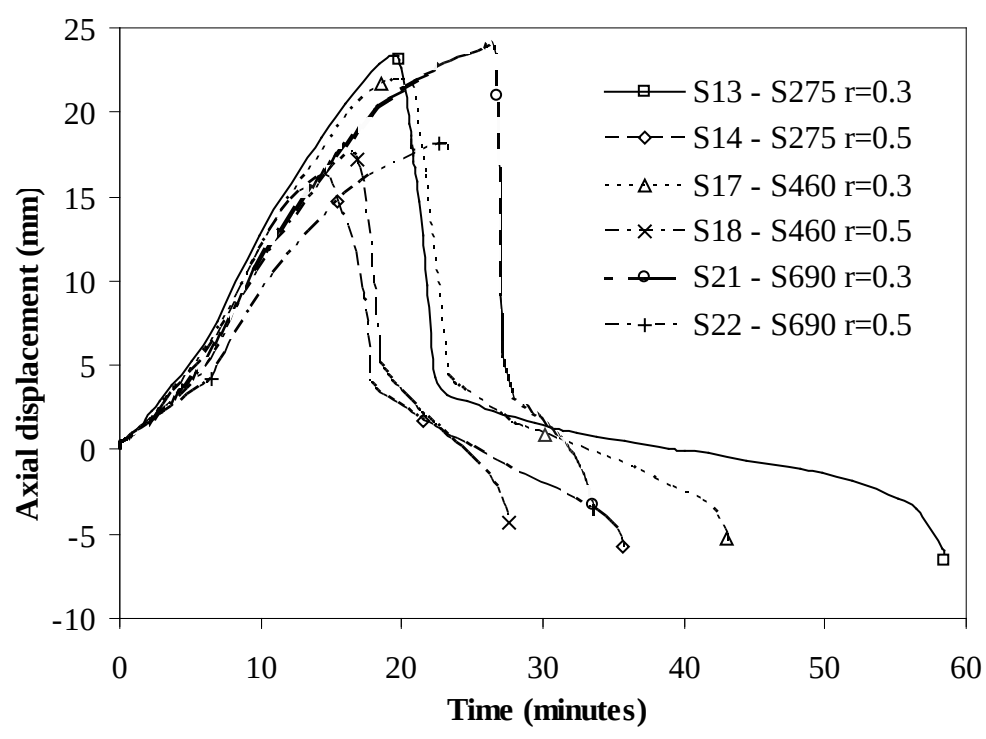

Fig. 10. Time-axial displacement relationships for S13, S14, S17, S18, S21 and S22

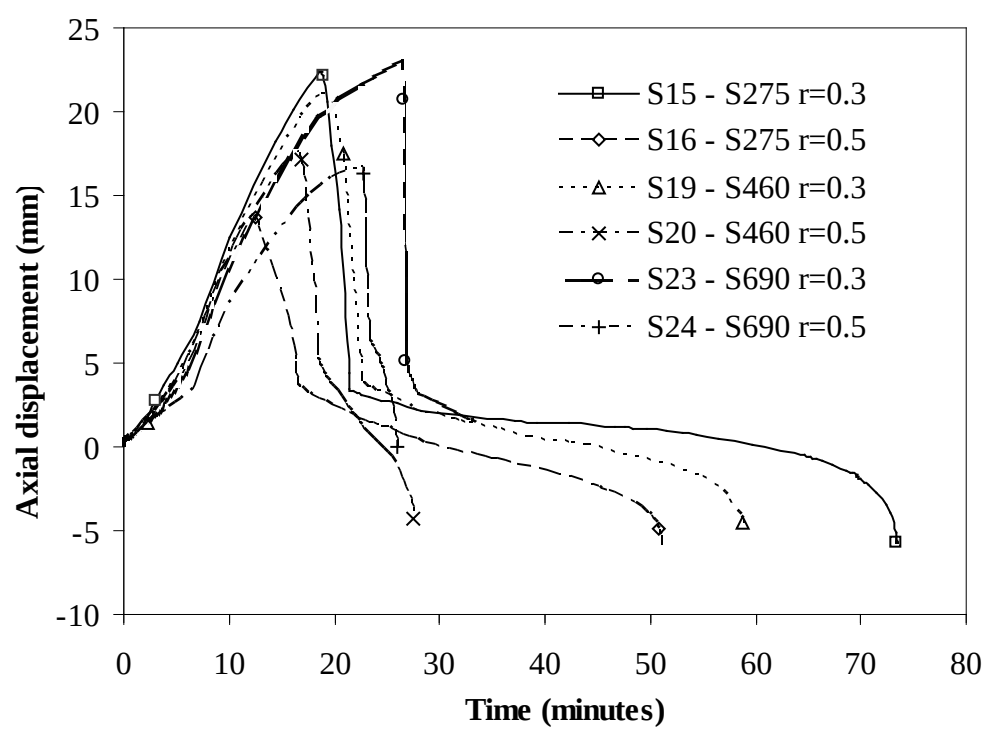

Fig. 11. Time-axial displacement relationships for S15, S16, S19, S20, S23 and S24

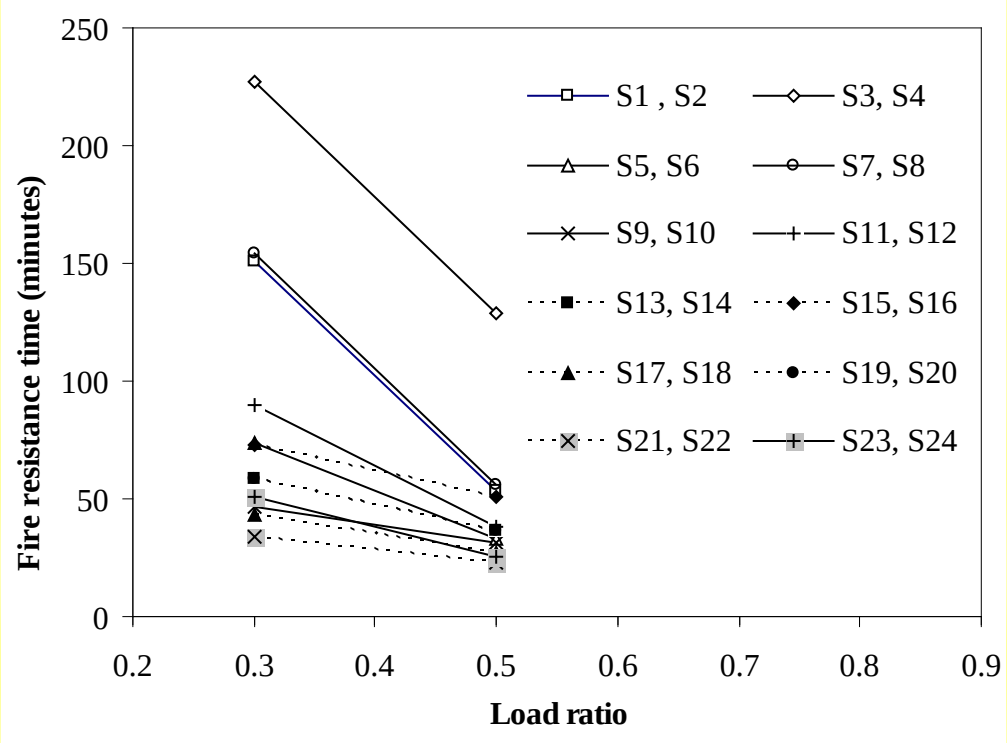

Fig. 12. Load ratio - fire resistance time relationships for G1 and G2

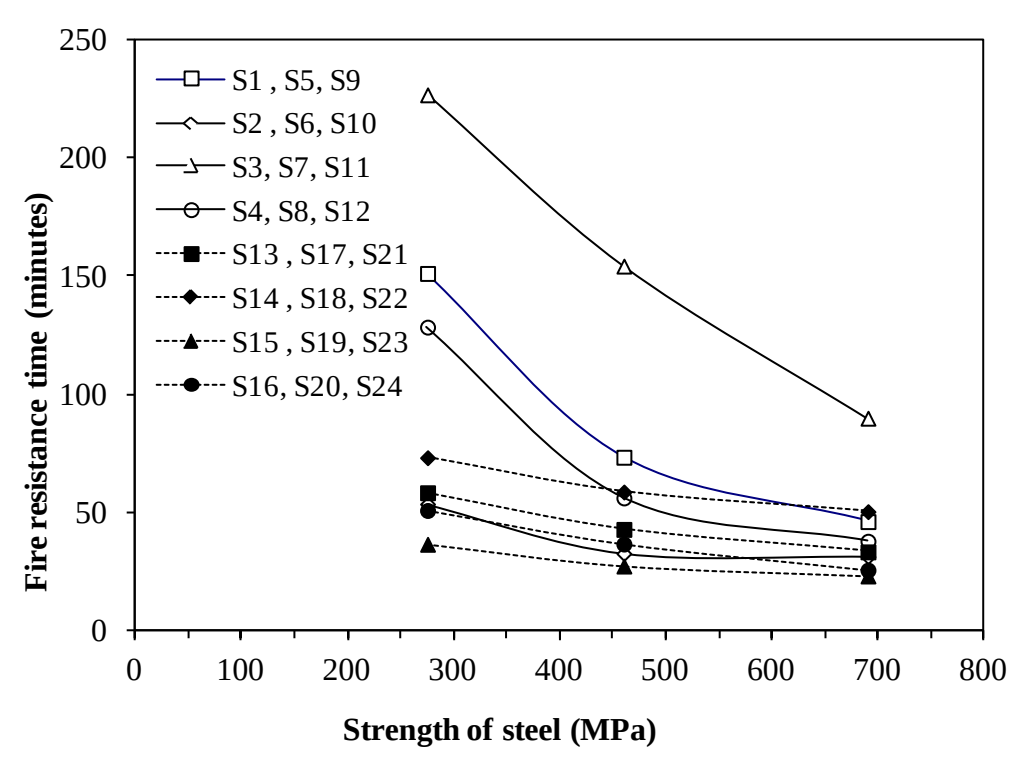

Fig. 13. Strength of steel- fire resistance time relationships for G1 and G2

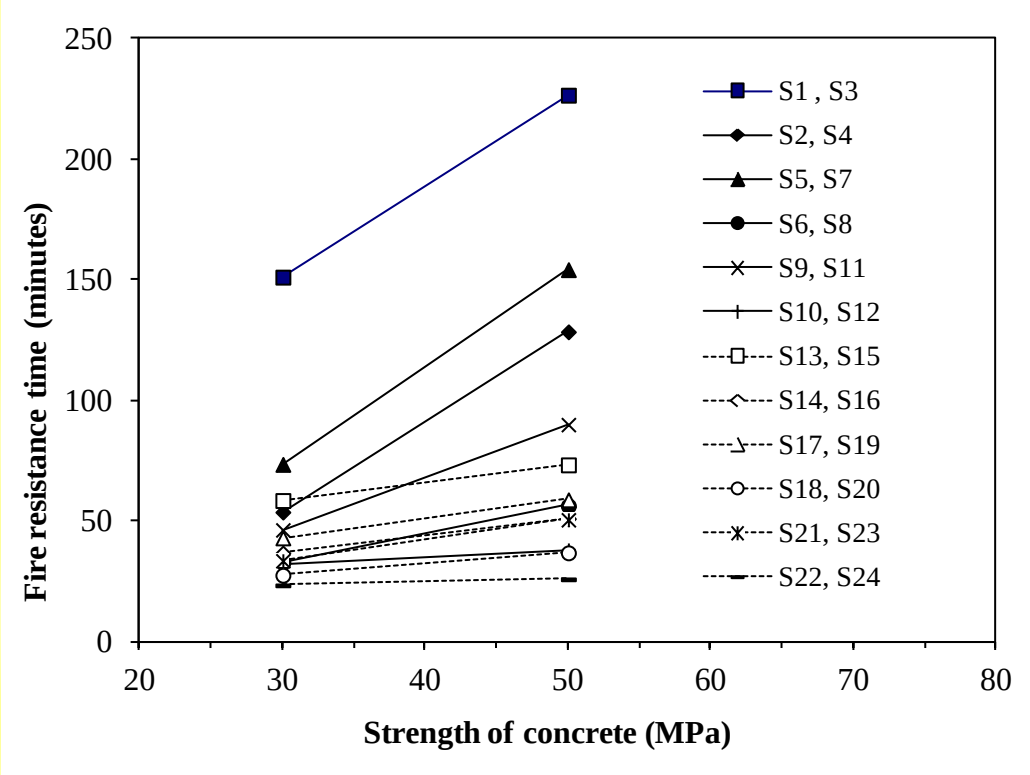

Fig. 14. Strength of concrete- fire resistance time relationships for G1 and G2

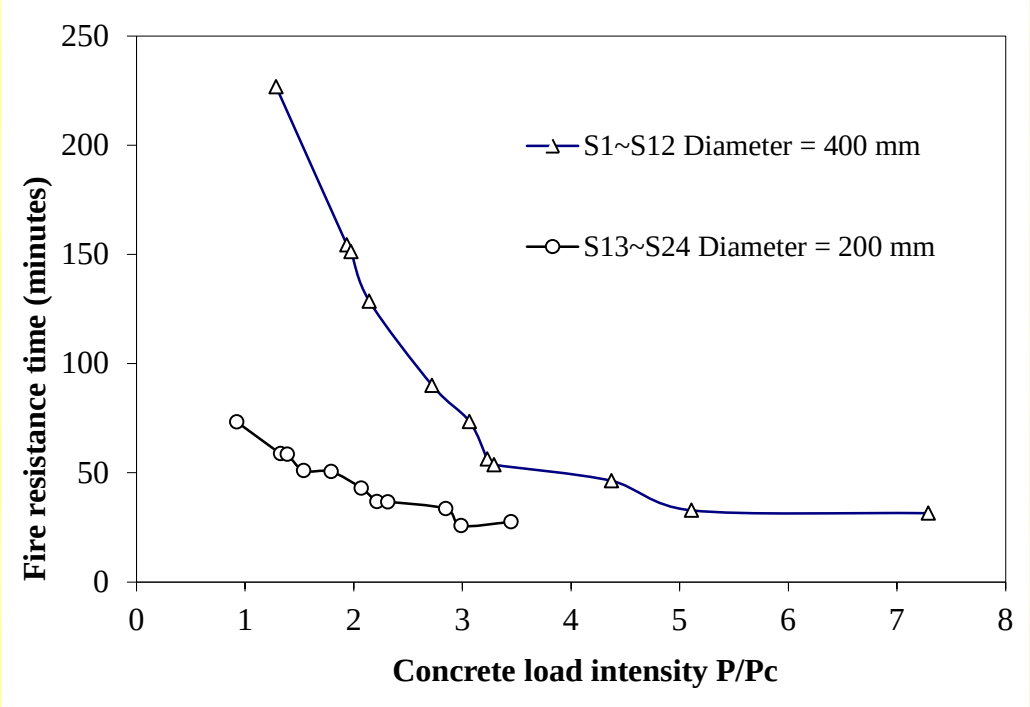

Fig. 15. Concrete load intensity- fire resistance time relationships for G1 and G2

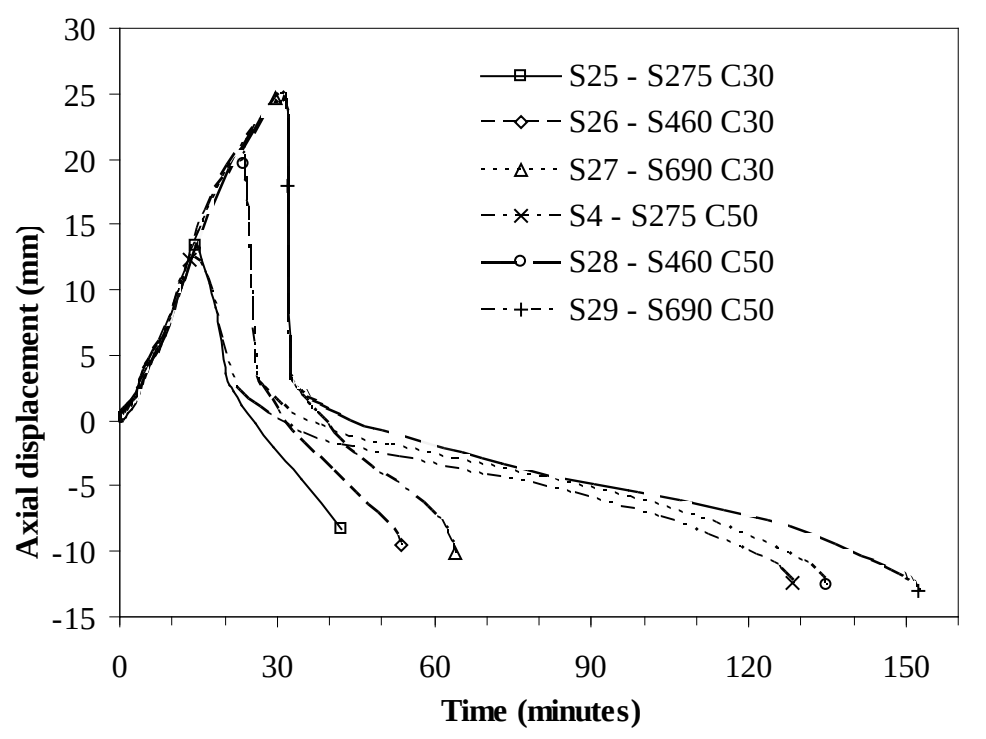

Fig. 16. Time-axial displacement relationships for G3 and S4 having the same load 2933 kN

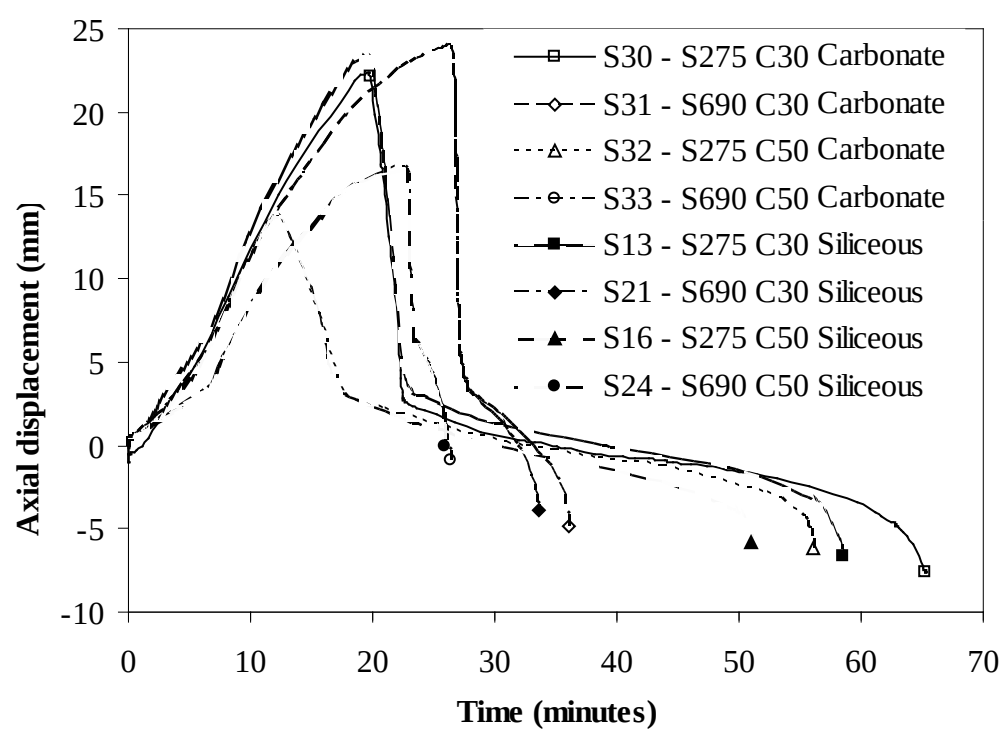

Fig. 17. Time-axial displacement relationships for G4, S13, S21, S16 and S24 to compare the effect of different aggregates

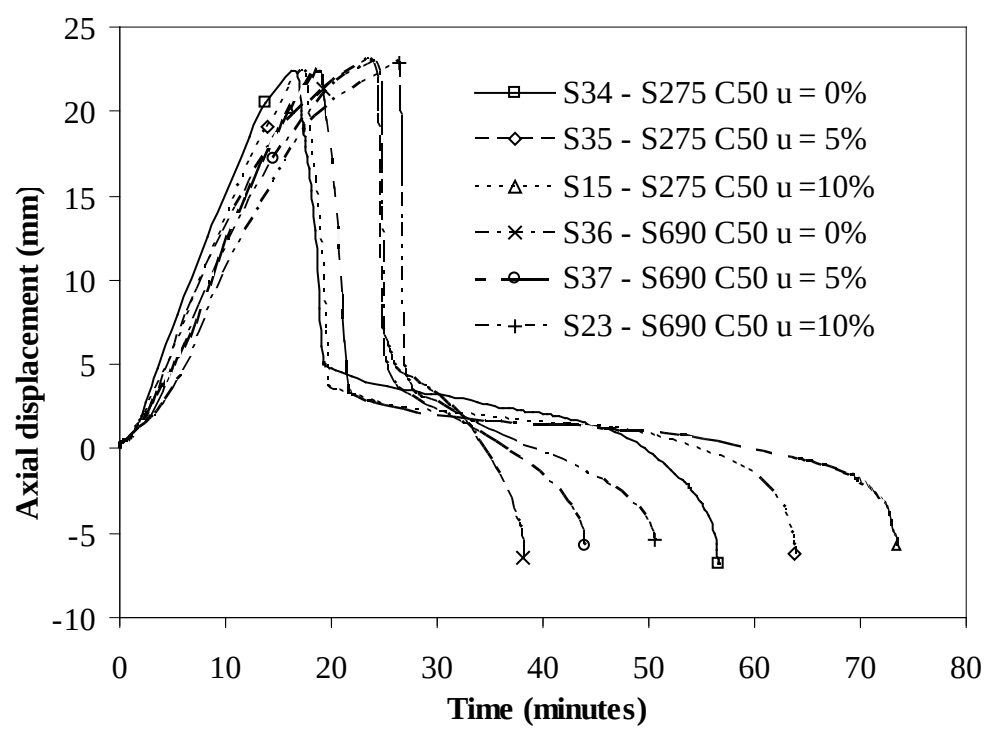

Fig. 18. Time-axial displacement relationships for G5, S15 and S23 to compare the effect of moisture content